Medicinal Chemistry Research (2019) 28:633–645
https://doi.org/10.1007/s00044-019-02318-4

MEDICINAL CHEMISTRY RESEARCH

ORIGINAL RESEARCH

Synthesis and biological evaluation of phenyl-amino-pyrimidine and indole/oxindole conjugates as potential BCR-ABL inhibitors

Abdul Rahim[1,2] · Riyaz Syed[1,3] · Y. Poornachandra[4] · M. Shaheer Malik[5] · Ch. Venkata Ramana Reddy[3] · Mallika Alvala[6] · Kiran Boppana[7] · B. Sridhar[8] · Ramars Amanchy[4] · Ahmed Kamal[1,6,9]

Received: 22 October 2018 / Accepted: 16 February 2019 / Published online: 16 March 2019

Abstract

Indole/isatin conjugated phenyl-amino-pyrimidine derivatives have been synthesized, characterized and evaluated in vitro for their potential as BCR-ABL inhibitors. Among the series, all derivatives (**7a**–**7o**) were found to be more cytotoxic than standard Imatinib against K-562 cell line. Compound **7l** was the most active in the series with almost two folds more potency than imitanib (IC_{50} 0.65 µM). In vitro enzymatic studies with recombinant ABL kinase enzyme exhibited promising inhibition in the range of 30–71 µM for most of these novel conjugates. In addition, modelling and other computational studies have been carried out to draw insight into the BCR-ABL protein interactions with the target molecules and drug like properties of the conjugates, respectively.

Graphical Abstract

Synthesis and biological evaluation of phenyl-amino-pyrimidine and indole/oxindole conjugates as potential BCR-ABL inhibitors.

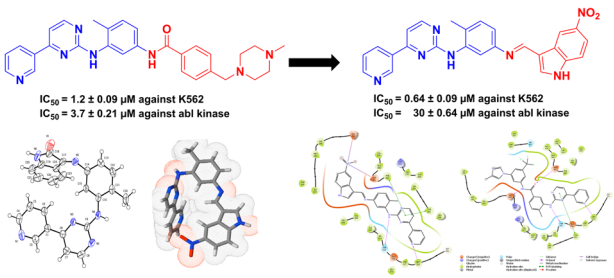

These authors contributed equally: Abdul Rahim, Riyaz Syed

Supplementary information The online version of this article (https://doi.org/10.1007/s00044-019-02318-4) contains supplementary material, which is available to authorized users.

✉ Ahmed Kamal
abdulrahimakot@gmail.com

[1] Medicinal Chemistry and Biotechnology Division, CSIR-Indian Institute of Chemical Technology (IICT), Hyderabad 500 007, India

[2] Academy of Scientific and Innovative Research, New Delhi 110 025, India

[3] Department of Chemistry, J.N.T. University, Kukatpally, Hyderabad 500 085, India

[4] Division of Applied Biology, CSIR-Indian Institute of Chemical Technology, Tarnaka, Hyderabad 500 085, India

[5] Central Research Laboratory and Department of Chemistry, Faculty of Applied Sciences, Umm Al-Qura University, 21955 Makkah, Saudi Arabia

[6] Department of Medicinal Chemistry, National Institute of pharmaceutical Education and Research (NIPER), Balanagar, Hyderabad 500 037, India

[7] GVK Bio Sciences Pvt. Ltd., Plot No. 79, IDA, Mallapur, Hyderabad 500076, India

[8] X-ray Crystallography Division, CSIR-Indian Institute of Chemical Technology, Hyderabad 500007, India

[9] School of Pharmaceutical Education and Research, Jamia Hamdard, New Delhi 110062, India

Keywords Phenyl-amino-pyrimidine · Indole · Oxindole · Bcr-Abl inhibitors · Chronic myeloid leukemia

Introduction

Tyrosine kinases (TKs) are the enzymes responsible to initiate transfer of phosphate group from ATP to tyrosine, a critical process in cellular machinery, and inhibition of TKs is currently considered as one of the most significant molecular targets in cancer drug discovery programs (Staquinini et al. 2015; Wilhelm et al. 2004). Chronic myeloid leukemia (CML) is a myelo-proliferative disorder associated with the philadelphia chromosome, resulting in the BCR-ABL fusion gene. This genetic abnormality results in the formation of a unique gene product (BCR-ABL), which is a constitutively active TK that is implicated in the development of CML (Salesse and Verfaillie 2002; An et al. 2010; Goldman and Melo 2008; Rebecca et al. 2018; Zámečníkova 2010; Carter et al. 2016). The phenylamino pyrimidine scaffold based BCR-ABL inhibitor, imatinib drug is considered as a "gold standard" in the treatment of patients with newly diagnosed CML (Fig. 1) (Karl Peggs and Stephen Mackinnon 2003; Nida and Naveed 2014; Druker 2003). However, the emergence of resistance against imatinib in association with BCR/ABL1 mutations (Sawyers et al. 2002; Talpaz et al. 2002; Azevedo et al. 2017; Valent 2007; O'Hare et al. 2007; Jabbour et al. 2009) has become a challenge. Further second generation BCR-ABL inhibitors such as nilotinib (Fig. 1), dasatinib, and ponatinib have been developed for treating the CML patients (Cortes et al. 2011, 2016; Hochhaus et al. 2008, 2016; Milojkovic et al. 2012; Porkka et al. 2008; Hughes et al. 2009; Kantarjian et al. 2007; Shah et al. 2014; Giles et al. 2013; Gambacorti-Passerini et al. 2014; Kantarjian et al. 2014; Nicolini et al. 2017; Lipton et al. 2016).

Similarly, another phenylamino pyrimidine derivative NRC-AN-019 is in phase-II clinical trials for treating CML and solid tumors (Second-line therapy). However, the common adverse effects of these marketed drugs include skin rash, nausea, vomiting, and vascular adverse events (VAEs) often leading to severe organ damage (Amala et al. 2013; Płużański and Piórek 2016; Valent 2011; Oren et al. 2015; Haguet et al. 2017; Herrmann 2016; Jason 2017; Ateyya et al. 2017; Sodergren et al. 2014). Furthermore, the third generation BCR-ABL inhibitors ponatinib is associated with certain arterial occlusive events (Dahlen et al. 2016; Jonathan et al. 2016; Chatree et al. 2016; Gusarova and Turkina 2016) and being approved by FDA with a black box warning.

Hence, there is a need to develop novel BCR-ABL inhibitors with enhanced drug safety and efficacy. Design of imatinib based novel BCR-ABL inhibitors offers opportunity of simpler, safer, and affordable therapeutics with lesser side effects and possessing unique inhibitory mechanisms which could address the issue of drug resistance.

On the other hand, indole and isatin are promising moieties in the design of anti-cancer agents and they are present in different anticancer drugs (Sidhu et al. 2015; El Sayed et al. 2015; Prakash et al. 2018; Vine et al. 2009, 2013; Havrylyuk et al. 2011; Teng et al. 2016). Keeping this in view, we envisaged hybridizing the promising phenylamino pyrimidine and indole/oxindole scaffolds into a single chemical entity and explore the biological effect exerted by these conjugates as newer BCR-ABL inhibitors. In our investigative strategy the amide moeity present in imatinib is substituted with isatin/indole ring through a bridging imine bond to afford new series of phenyl-amino-pyrimidine and indole/oxindole conjugates. This was followed by the evaluation of the therapeutic potency of these conjugates against K-562 cancer cell line and recombinant ABL kinase enzyme with comparison to standard drug

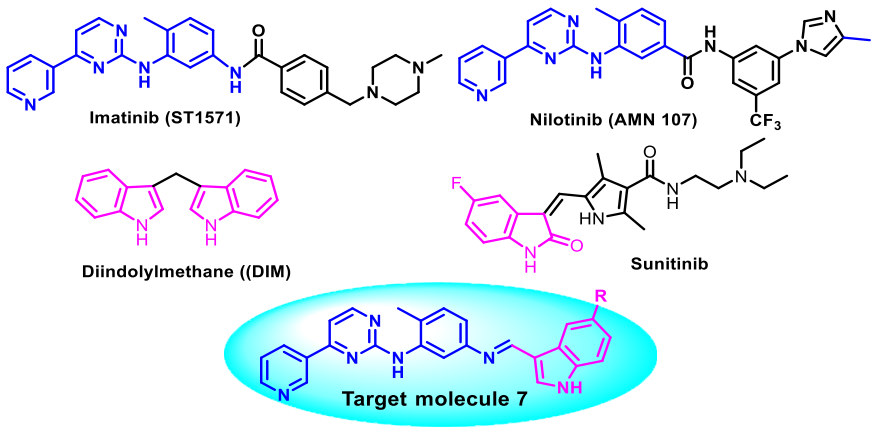

Fig. 1 BCR-ABL inhibitors and Indole/oxindole based inhibitors

Scheme 1 Synthesis of phenylamino pyrimidine intermediate **6**

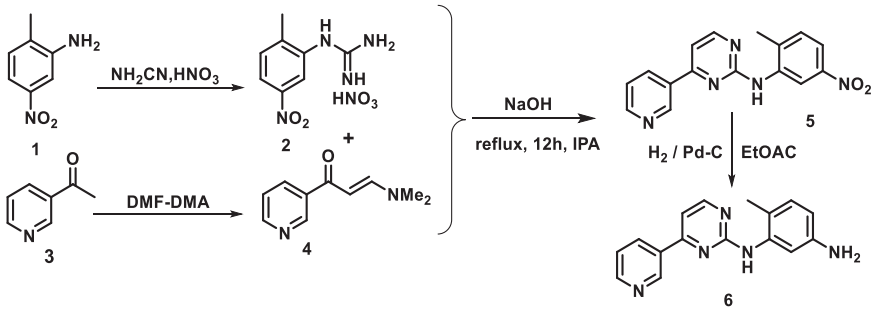

Table 1 Optimization of the reaction conditions

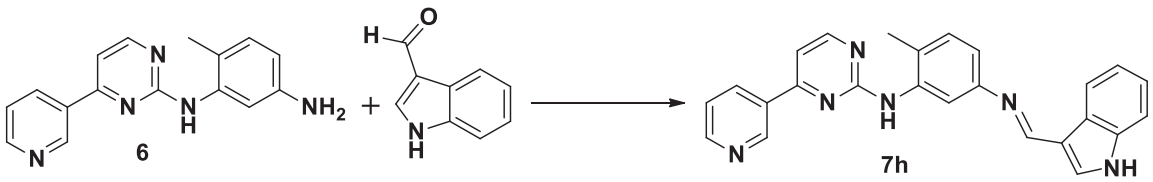

Entry	Solvent	Catalyst	Temp (°C)	Time (h)	Yield[b] (%)
1	H_2O	–[a]	30	16	10
2	H_2O	AcOH	40	8	30
3	MeOH	AcOH	30	8	55
4	MeOH	AcOH	60	4	85
5	MeOH	–[a]	60	4	90
6	EtOH	AcOH	80	8	75
7	DCM	AcOH	40	8	44

[a]No catalyst used

[b]Isolated yield

imatinib. Furthermore, we studied the BCR-ABL protein binding interactions and drug like properties of these newly synthesized ligands.

Results and discussion

Chemistry

The chemical strategy for the synthesis of the intermediate amine **6** started with the condensation of 5-nitro-2-methyl aniline (**1**) with cynamide to furnish the guanidine derivative (**2**), followed by reaction with pyridine based chalcone (**4**) in the presence of inorganic base to afford pyrimidine derivative (**5**). The pyridine chalcone (**4**) was obtained from 3-acetyl pyridine (**3**). The catalytic reduction of pyrimidine derivative **5** with hydrogen on Pd/carbon in ethyl acetate afforded the desired intermediate **6** (Scheme 1) (Zimmermann 1993, 1996; Zimmermann et al. 1996).

Upon synthesizing **6**, we proceeded towards the synthesis of the target compounds through imine formation. In order to achieve this, reaction between compound **6** and indole-3-carboxaldehyde was first carried out in water at room temperature and 40 °C, the progress of the reaction was monitored by TLC, however the starting materials were not completely consumed even until 16 h which is in turn affected the product yield (Table 1, entry 1). Therefore, a focused optimization study was carried out with different solvents in the presence and absence of acetic acid as catalyst at varying temperature. It was observed that the use of catalytic amount of acetic acid afforded better yields of the product in water (Table 1, entry 2). On switching from water to methanol in the presence of catalytic acetic acid at room temperature the yield of the reaction improved to 55% (Table 1, entry 3) and with the increase of the temperature to 60 °C, the yield further improved to 85% with reduced reaction time (Table 1, entry 4). Interestingly, when the reaction was performed in methanol without catalytic acetic acid at 60 °C the yield was slightly better (Table 1, entry 5). Furthermore the reaction was also performed in ethanol and dichloromethane, however the yields decreased compared to methanol (Table 1, entries 6–7).

Scheme 2 Reaction between intermediate amine (**6**) with isatin and aldehyde

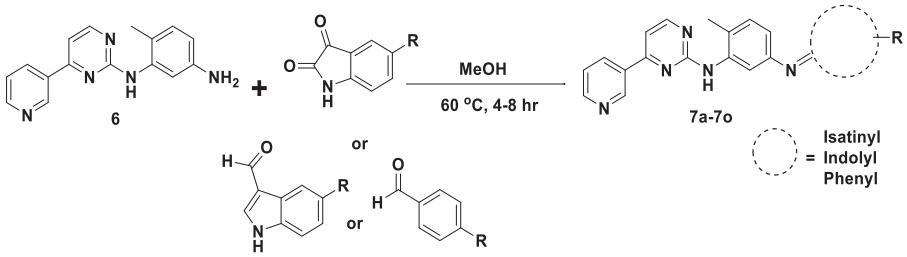

Table 2 Synthesis of Imatinib based analogues

Entry	R	Time (h)	Yield (%)
7a	H	5	80
7b	Cl	4.5	85
7c	F	4	75
7d	Br	5.5	69
7e	I	6	85
7f	Me	7	80
7g	MeO	7.5	70
7h	H	6	74
7i	F	4.5	82
7j	Cl	5	84
7k	CN	5	70
7l	NO_2	4	74
7m	MeO	6	72
7n	CF_3	6	85
7o	F	6	75

Hence, we performed the condensation reaction of intermediate **6** with different isatins and aldehydes under the optimized reaction conditions with methanol as solvent at 60 °C to provide the desired conjugates **7a**–**7o** as outlined in Scheme 2. Equimolar mixture of compound **6** and different isatins or aldehydes taken in methanol (5 ml) stirred at 60 °C temperatures for 4–8 h furnished the desired compounds in good to excellent yield (Table 2). Since this kind of condensation reactions moves in the forward direction with progressive removal of water, we carried out the reaction with Dean and Stark apparatus with different water immiscible solvents, however no remarkable changes were observed in the yields and time.

The structures of the final compounds were confirmed based on their ^{1}H, ^{13}C NMR and HRMS data. In case of compound **7a** and **7b**, we observed three singlet peaks in ^{1}H NMR spectra for isatinyl, pyridiny,l and secondary amine protons at chemical shifts (δ) values of 10.85, 9.13, 8.64 and 11.07, 9.18, 8.93 respectively as well as in ^{13}C NMR characteristic peaks for compound **7a** and **7b** at δ 164.25, 163.72 for carbons directly attached to the three nitrogen, at δ 161.89, 162.00 for carbons attached to imine bond, at δ 161.17, 161.23 for carbons attached to nitrogen of pyridine ring and at δ 155.16, 154.03 for amide carbon respectively. Moreover to further support the characterization of these new conjugates, X-ray crystallography was performed with compound **7a**, which clearly identified the presence of pyridine, pyrimidine and oxindole rings as well as the imine bond with precision (Fig. 2).

Biological evaluation

Inhibition of cell proliferation

To assess the potency of the novel conjugates of imitanib (**7a**–**7o**), we evaluated their effects on cell proliferation (Hamaï et al. 2006) as well as enzymatic activity with imatinib drug as a reference. The decrease in cell viability of K-562 cells treated with the compounds **7a**–**7o** for 48 h assessed with the in vitro SRB assay (Kasinski et al. 2015; Skehan et al. 1990; Vichai and Kirtikara 2006) revealed their promising anti-proliferative activity. All the derivatives of the series (**7a**–**7o**) exhibited more potent cytotoxicity than imatinib against K-562 cell line in the range of 0.65–1.1 μM (Fig. 3). Compound **7l** with indole ring exhibited the best activity in the series with an IC_{50} value of 0.65 μM and almost two folds more potency than imitanib. We believe introduction of XXX groups and specifically XYY groups in ZZZ molecules enhanced their binding to the kinase in focus and thus inhibiting cell proliferation. Hence, to test the Abl kinase activity we consequently performed in vitro kinase assays (Mow et al. 2002).

Enzymatic kinase activity

In this study, all the compounds (**7a**–**7o**), were tested by in vitro assay against the recombinant ABL kinase enzyme (Ding et al. 2008; Ouellette et al. 2016). Most of them displayed good anti-enzymatic activity with IC_{50} value arranging from 30 to 71 μM, however under our experimental conditions, imatinib drug showed a nine fold better IC_{50} value. This indicates that there may be other molecular targets where these compounds could bound and provides better cytotoxicity values than imatinib. Further, compounds **7a**, **7h**, **7n**, and **7o** showed no significant inhibitory activity toward ABL ($IC_{50} > 100$ μM). Amongst the identified human kinome of 518 protein kinases many have been identified to bind to same inhibitors thus ensuing

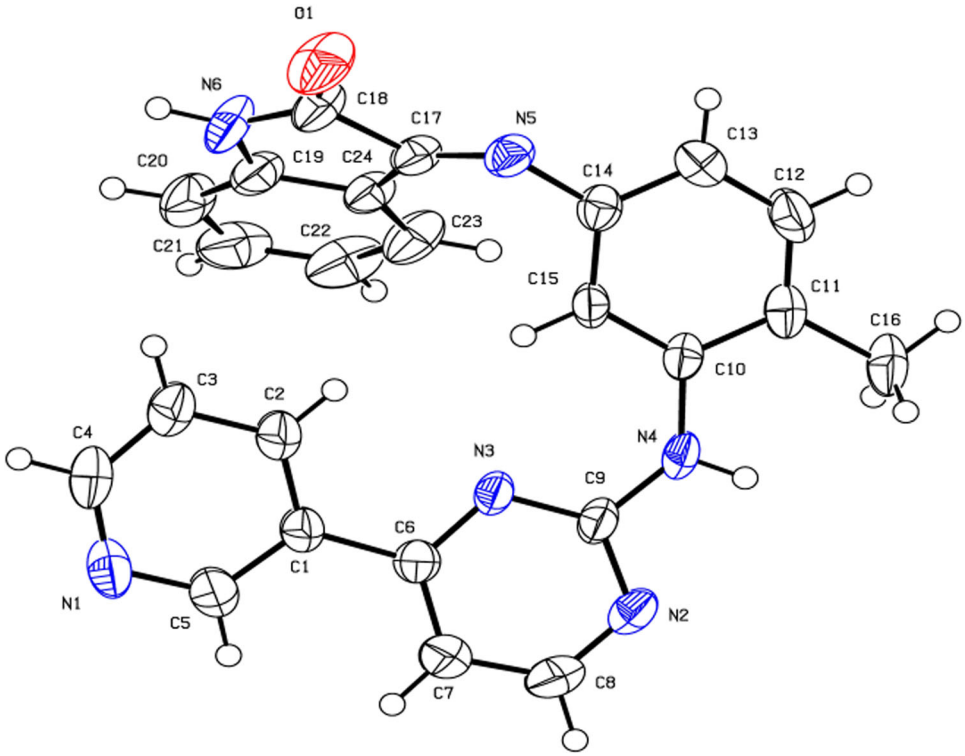

Fig. 2 A view of **7a**, showing the atom-labeling scheme. Displacement ellipsoids are drawn at the 30% probability level and H atoms are represented by circles of arbitrary radii

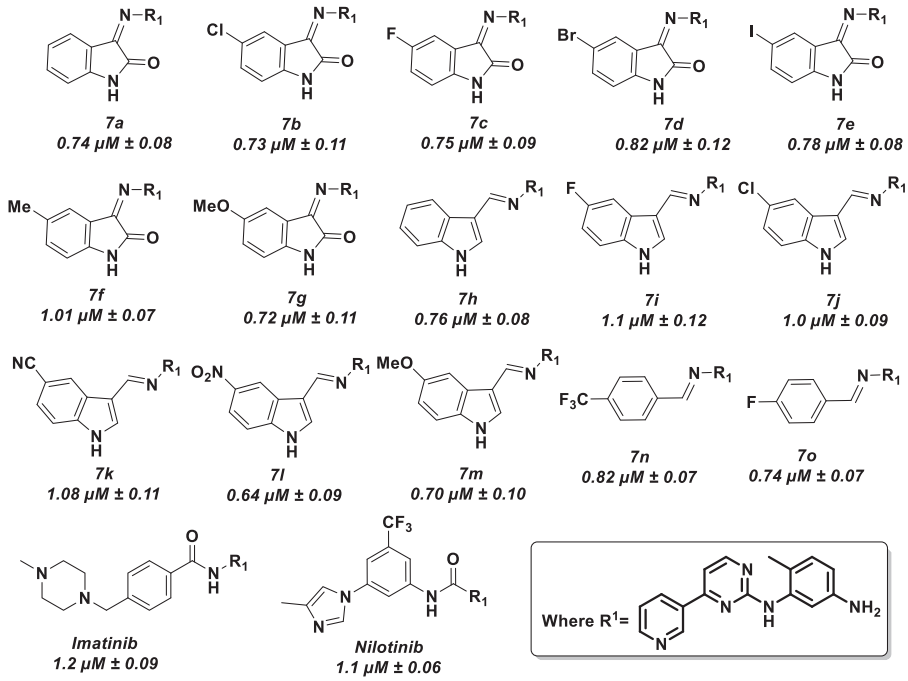

Fig. 3 In vitro cytotoxicity against K562 cell line

polypharmacology (Manning et al. 2002). It has already been known that kinase inhibitors show less promiscuity towards their targets owing to their binding of homologous ATP-binding sites in multiple freely available cellular kinases. However their promiscuity is to be seen as rationalized due to their ability to bind to the same region of several known protein kinases (Hu et al. 2017).

Structure activity relationship (SAR) can be explained on the basis of values obtained from the cytotoxicity and anti-enzymatic profile of compounds (**7a**–**7o**), (Fig. 3 and Table 3). Interestingly, compounds having oxindole (**7a**–**7g**) were found most active amongst the series; however there was no remarkable distinction in activity between electron donating and withdrawing groups containing

Table 3 In vitro bcr-abl enzymatic activity

Compounds	IC_{50} (μM)
7a	>100
7b	60 ± 0.58
7c	62 ± 0.64
7d	71 ± 0.66
7e	55 ± 0.42
7f	40 ± 0.51
7g	36 ± 0.38
7h	>100
7i	55 ± 0.49
7j	37 ± 0.28
7k	40 ± 0.36
7l	30 ± 0.64
7m	52 ± 0.32
7n	>100
7o	>100
Imatinib	3.7 ± 0.21

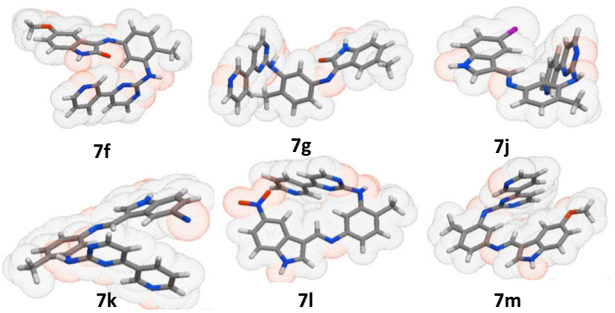

Fig. 4 Topological polar surface area (TPSA) of the top active synthesized molecules

compounds. Nevertheless, methyl group slightly decreases the activity with IC_{50} value 1.01 μM in compound **7f**. In case of indolyl compounds (**7h**–**7m**), electron rich indoles have shown good activity however, halogenated and electron deficient indoles decreases the activity with an exception of nitro compound **7l** which has shown excellent activity with IC_{50} value 0.65 μM. Furthermore, aromatic compounds (**7n**–**7o**), were found to have relatively similar cytotoxicity as that of oxindole analogues (**7a**–**7g**) (Fig. 4). In case of enzymatic activity, the oxindole analogues (**7a**–**7g**) having electron donating groups namely methyl and methoxy have shown better activity than electron withdrawing groups. However, in case of indole based derivatives (**7h**–**7m**), electron deficient groups were found to be better, particularly compound **7l** with IC_{50} value 30 μM. None of the aromatic compounds (**7n**–**7o**) were found to have anti-enzymatic activity.

Traditionally, oxindole extracted from the cat claw's plant *Uncaria tomentosa* in Amazon South America, have demonstrated vast therapeutic potential. The extent of pharmacological activities ascribed to oxindole derivatives, include anti-cancer, anti-viral anti-leishmanial, antibacterial, antidiabetic, antioxidant, AChE inhibitory, adrenergic receptor agonistic, analgesic, spermicidal, vasopressin/progesterone antagonistic, neuroprotection, and NMDA blocker activities (Kaur et al. 2016). Oxindole derivatives have gained respect in the field due to the principal compound Sunitinib, that has been made for inhibition of VEGFR2 specifically as an anti-angiogenesis compound (Kang et al. 2016) that has been clinically approved for renal cell carcinoma. Oxindole derivatives have been shown to bind to ATP-binding region of the catalytic domain of kinases.

Table 4 Drug-likeness properties of the top six active indole based scaffolds

Compound	TPSA score	miLogP	H-bond acceptors	H-bond donors
7f	95.93	5.03	7	2
7g	105.16	4.64	8	2
7j	78.86	5.64	6	2
7k	102.65	4.72	7	2
7l	124.68	4.92	9	2
7m	88.09	5.02	7	1

Druglikeness, toxicity and pharmacokinetic toxicity and pharmacokinetics analysis

The pharmacokinetics and drug-likeness properties of the hit compounds were studied using Mol-inspiration and Swiss ADME online server by submitting SMILES. The compounds were filtered out based on Water Partition Coefficient (miLogP) values to be <5 which predict lower toxicity, possible oral administration and non-specific binding. The TPSA (Topological Polar Surface Area) score <140 A^0 (da Silva et al. 2015) indicating a high possibility of absorption (Table 4). In addition, the compounds were also analyzed for bioavailability property using Swiss ADME (Daina et al. 2017a, b) (Figs 4 and 5).

The pharmacokinetic and physicochemical properties of all the synthesized compounds were studied using Swiss ADME server. Among all the tested, five molecules were selected as hit molecules by passing the filtering criteria of miLogp < 5 and TPSA < 140 A^0. BOILED-Egg (Brain Or IntestinaL EstimateD permeation method) is a perceptive model to predict the passive gastrointestinal absorption (HIA) and Blood Brain Barrier (BBB) permeation of small molecules (Daina et al. 2017a, b). The BOILED-Egg analysis showed that most of the molecules (11 compounds) are highly absorbable in the gastrointestinal tract. The active efflux mechanism, P-gp as substrate has involved in the

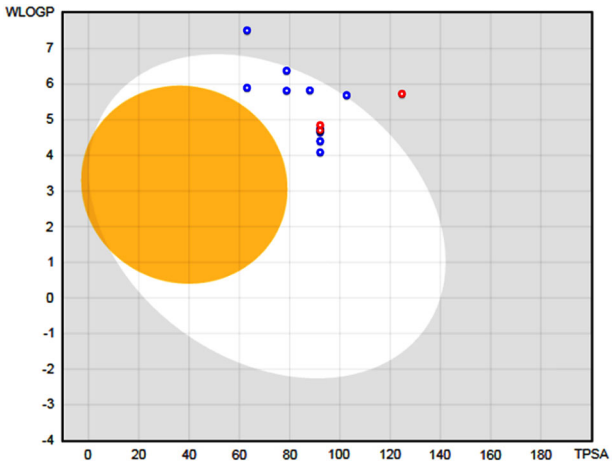

Fig. 5 Brain/intestinal permeation estimation

permeation of molecules (indicated as blue dots) to the gastrointestinal lumen (Fig. 5).

Molecular docking studies

The molecular docking studies of **7h–7m** designed inhibitors demonstrated binding into the pocket of BCR-ABL enzyme and forming one H-bond with the hinge region Met-318 of Abl kinase catalytic domain, proven to be essential for the inhibition of kinase activity (Parcha et al. 2017; Banavath et al. 2014). Critical analysis of the ligand interaction pattern revealed that nitrogen of pyridyl ring system involved in a H-bond with Met-318. The –NH linker showed a H-bond with Tyr 315 and pyramidal ring exhibited strong Π-Π stacking with Thr 253 as shown in supplementary data with all synthesized molecules. Further formation of salt bridge between Glu286, Asp 381 amino acids and nitro substitution on indole moiety of compound **7l** contributed for BCR-ABL inhibition and absent in other derivatives. Interaction with Glu286, Asp 381 is an essential interaction to show Bcr-Abl inhibition as suggested and evidenced by Parcha et al. (2017) and also observed with co-crystal ligand, nilotinib (Sabitha 2012) (Fig. 6).

From in vitro enzymatic and in silico studies it is evidenced that only compound **7l** making interaction with Glu286 and Asp 381 inhibited the BCR-ABL with an IC_{50} of 30 µM and arrested the K-562 cell growth with an IC_{50} of 0.64 ± 0.09 demonstrating the potential lead like properties of **7l** to treat CML (Fig. 6).

It was observed that nilotinib formed hydrogen bonds with Asp-381 and Glu-296 where as the compound **7l** did not formed these hydrogen bonds and this will be making the compound more drug like as breaking the H-bonds needs more energy making it physiologically non favorable for the active site. Yet, the nitro group of the indole moiety in **7l** forms stable salt bridges with Asp-381 and Glu-296. We confer that **7l** may look as potential scope for lead development.

Conclusion

Synthesis, characterization and in vitro evaluation of indole/isatin conjugated phenyl-amino-pyrimidine derivatives as potential BCR-ABL inhibitors have been demonstrated. Among the series, all derivatives (**7a–7o**) were found to be more cytotoxic than standard Imatinib against K-562 cell line. Notably, compound **7l** was the most active in the series with almost two folds more potency than imitanib (IC_{50} 0.65 µM). Furthermore, in vitro enzymatic studies with recombinant ABL kinase enzyme exhibited promising inhibition in the range of 30–71 µM for most of these novel conjugates. In addition, modelling and other computational studies have been carried out to draw insight into the BCR-ABL protein interactions with the target molecules and drug like properties of the conjugates, respectively. A detailed study in understanding pattern of this biological activity outcome would be worthwhile research investigation.

Experimental section

Chemistry

All reagents, starting materials, and solvents were purchased from Aldrich (Sigma-Aldrich, St. Louis, MO, USA) or Alfa Aesar (Johnson Matthey Company, Ward Hill, MA, USA) and used without further purification. Reactions were monitored by TLC, performed on silica gel glass plates containing 60 F-254, and visualization on TLC was achieved by UV light or using an iodine indicator. Column chromatography was performed with Merck 60–120 mesh silica gel. ^{1}H and ^{13}C NMR spectra were recorded with 75, 100, 300, 400, and 500 MHz spectrometer in $CDCl_3$ and DMSO-d_6 solutions. Chemical shifts (δ) are expressed in ppm relative to the internal standard TMS and multiplicities of NMR signals are represented as singlet (s), broad singlet (bs), doublet (d), triplet (t), double doublet (dd), triplet of doublet (td), and multiplets (m). High-resolution mass spectra (ESI-HRMS) were obtained by using ESI-QTOF mass spectrometer. Melting points were determined on an electro-thermal melting point apparatus and are uncorrected.

General procedure for the synthesis of compounds (7a–7o)

6-methyl-N^1-(4-(pyridin-3-yl)pyrimidin-2-yl) benzene-1,3-diamine (compound **6**) (0.5 mmol) and 5-substituted, indoline-2,3-dione(isatins) or indole and aromatic aldehydes (0.5 mmol) were taken in methanol (5 ml) and stirred at 60 °C temperature for 4–8 h. The reaction was monitored by

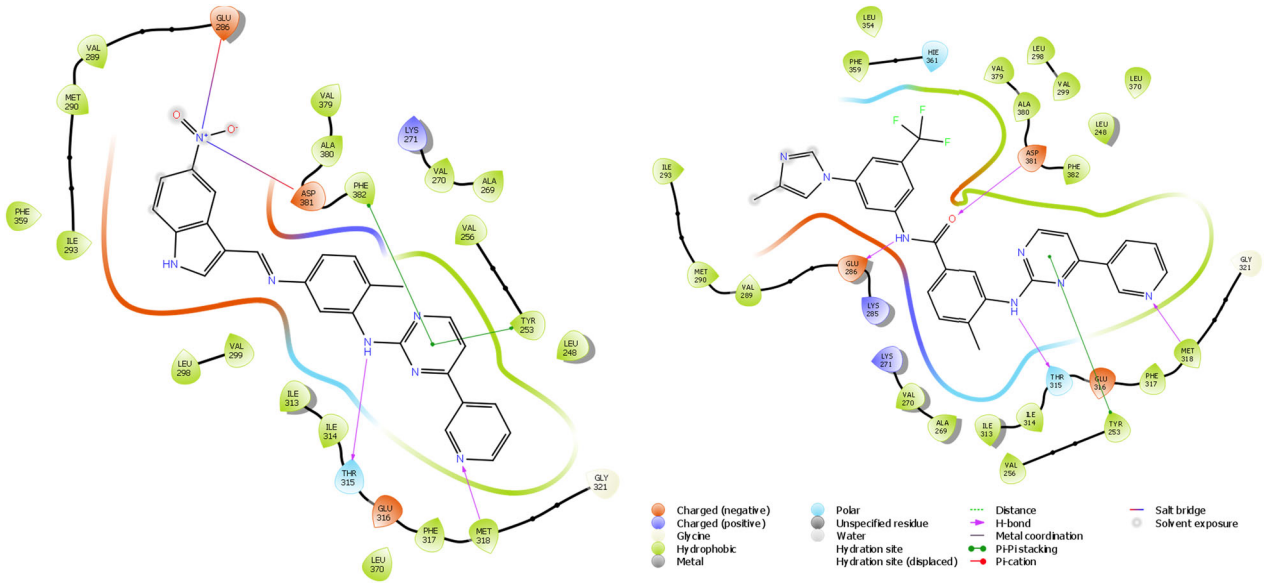

Fig. 6 Binding pose of **7l** and nilotinib into the active site pocket of BCR-ABL enzyme

TLC using methanol and chloroform (2%) as a solvent system. After completion of reaction this mixture was evaporated by vacuum distillation and the residue was extracted with ethyl acetate (25 mL × 3). The organic solution was dried over anhydrous Na_2SO_4 and evaporated the solvent to offered crude product. This was further purified by column chromatography using 0.1:10 methanol/chloroform as eluent to obtain the pure compound in good yield.

(*Z*)-3-((4-Methyl-3-((4-pyrdin-3-yl) pyrimidin-2-yl) amino-phenyl) imino) indolin-2-one (7a) White solid (80%); R_f: 0.35 (5%, MeOH/$CHCl_3$); M.P.**:** 254-255 °C; ^{1}H NMR (300 MHz, $CDCl_3$ + DMSO-d_6) δ 10.85 (s, 1H), 9.13 (s, 1H), 8.64 (s, 1H), 8.57 (d, J = 3.9Hz, 1H), 8.40 (d, J = 4.9Hz, 1H), 8.20 (d, J = 7.7 Hz, 1H), 7.37 (s, 1H), 7.29–7.16 (m, 4H), 6.82 (dd, J = 12.5, 7.8 Hz, 2H), 6.62 (dd, J = 16.5, 8.2 Hz, 2H), 2.32 (s, 3H).; ^{13}C NMR (75 MHz, $CDCl_3$ + DMSO-d_6) δ 164.25, 161.89, 161.17, 159.25, 155.16, 151.25, 148.51, 148.23, 147.16, 138.90, 134.27, 132.44, 131.33, 127.99, 126.30, 123.60, 121.86, 115.98, 113.63, 113.39, 111.57, 107.90, 18.00. HRMS (ESI) calculated for $C_{24}H_{19}ON_6$ $[M+H]^+$ 407.1614; found: 407.1613.

(*Z*)-5-Chloro-3-((4-methyl-3-((4-pyrdin-3-yl) pyrimidin-2-yl) amino) phenyl) imino) indolin-2-one (7b) White solid (85%); R_f**:** 0.25 (5% MeOH/$CHCl_3$); M.P.**:** 252-253 °C; ^{1}H NMR (300 MHz, $CDCl_3$ + DMSO-d_6) δ 11.07 (s, 1H), 9.18 (s, 1H), 8.93 (s, 1H), 8.61 (d, J = 3.8Hz, 1H), 8.44 (d, J = 5.1Hz, 1H), 8.29 (d, J = 7.9 Hz, 1H), 7.32 (m, 5H), 6.88 (d, J = 8.4 Hz, 1H), 6.77 (s, 1H), 6.70 (d, J = 7.4 Hz, 1H), 2.34 (s, 3H); ^{13}C NMR (75 MHz, $CDCl_3$ + DMSO-d_6) δ 163.72, 162.00, 161.23, 159.42, 154.03, 151.42, 148.35, 147.90, 145.92, 139.08, 134.33, 133.86, 132.45, 131.50, 128.89, 125.95, 125.65, 123.71, 117.03, 113.78, 113.57, 113.12, 108.11, 18.11; HRMS calculated for $C_{24}H_{18}ON_6Cl$ $[M+H]^+$ 441.1225; found: 441.1225; $C_{24}H_{18}ON_6Cl$ $[M+2]^+$ 443.1196; found: 443.1236;

(*Z*)-5-Fluoro-3-((4-methyl-3-((4-pyrdin-3-yl) pyrimidin-2yl) amino) phenyl) imino) indolin-2-one (7c) White solid (75%); R_f: 0.28 (5% MeOH/$CHCl_3$); M.P.**:** 243–245 °C, ^{1}H NMR (300 MHz, $CDCl_3$ + DMSO-d_6) δ 10.78 (s, 1H), 9.08 (s, 1H), 8.54 (d, J = 3.9 Hz, 1H), 8.36 (d, J = 5.2 Hz, 1H), 8.17 (d, J = 8.0 Hz, 1H), 7.53 (s, 1H), 7.26–7.07 (m, 5H), 6.94–6.79 (m, 1H), 6.66–6.63 (m, 2H), 2.33 (s, 3H).; ^{13}C NMR (75 MHz, $CDCl_3$ + DMSO-d_6) δ 164.48, 162.68 (d, J_1 = 270.7 Hz, 1C), 158.97, 155.88, 154.41, 151.10, 148.16, 147.73, 143.22, 138.58, 134.30, 132.51, 131.29, 127.27, 123.48, 120.48 (d, J_2 = 26.5 Hz, 1C), 116.22 (d, J_3 = 7.8 Hz, 1C), 113.82, 113.35, (d, J_2 = 26.7 Hz, 1C), 112.37, 108.06, 17.89; HRMS (ESI) calculated for $C_{24}H_{18}ON_6F$ $[M+H]^+$ 425.1520; found: 425.1512.

(*Z*)-5-Bromo-3-((4-methyl-3-((4-pyrdin-3-yl) pyrimidin-2-yl) amino) phenyl) imino) indolin-2-one (7d) White solid (69%); R_f: 0.30 (5% MeOH/$CHCl_3$); M.P.: 194-196 °C; ^{1}H NMR (300 MHz, $CDCl_3$ + DMSO) δ 10.83 (s, 1H), 9.16 (s, 1H), 8.64 (d, J = 4.6 Hz, 1H), 8.48 (t, J = 4.4 Hz, 1H), 8.24 (d, J = 8.1 Hz, 1H), 7.82 (s, 1H), 7.77 (s, 1H), 7.59 (s, 1H), 7.34–7.28 (m, 2H), 7.19 (d, J = 5.1 Hz, 1H), 7.15 (s, 1H), 6.80 (t, J = 8.6 Hz, 1H), 6.74 (d, J = 7.7 Hz, 1H), 2.44 (s, 3H); ^{13}C NMR (75 MHz, $CDCl_3$ + DMSO) δ 163.2, 161.7, 160.9, 159.44, 153.7, 151.31, 148.1, 147.7, 145.9, 138.8, 136.5, 134.2, 132.3, 132.1, 131.3, 130.4, 128.8, 123.6, 119.5, 117.3, 113.5, 111.1, 107.9, 17.8; HRMS (ESI)

calculated for $C_{24}H_{18}ON_6Br$ $[M + H]^+$ 485.0720; found: 485.0748; $C_{24}H_{18}ON_6Br$ $[M + 2]^+$ 485.0700; found: 485.0727.

(Z)-5-Iodo-3-((4-methyl-3-((4-pyrdin-3-yl) pyrimidin-2-yl) amino) phenyl) imino) indolin-2-one (7e) White solid (85%); R_f: 0.40 (5% MeOH/$CHCl_3$); M.P.: 126-128 °C; ^{1}H NMR (300 MHz, $CDCl_3$ + DMSO-d_6) δ 10.91 (s, 1H), 9.09 (s, 1H), 8.54 (d, $J = 3.4$ Hz, 1H), 8.40 (d, $J = 5.2$ Hz, 1H), 8.17 (d, $J = 8.0$ Hz, 1H), 7.80 (d, $J = 2.8$ Hz, 1H), 7.57 (s, 1H), 7.45 (d, $J = 8.2$ Hz, 1H), 7.24 (d, $J = 8.0$ Hz, 1H), 7.17 (d, $J = 5.5$ Hz, 1H), 2.35 (s, 3H); ^{13}C NMR (75 MHz, $CDCl_3$ + DMSO-d_6) δ 163.74, 162.24, 162.06, 160.86, 159.24, 159.12, 153.56, 151.12, 148.23, 147.74, 146.58, 146.28, 145.86, 138.66, 134.51, 133.13, 132.61, 131.27, 130.77, 127.34, 123.75, 123.57, 117.91, 115.00, 113.85, 113.64, 112.26, 111.16, 110.11, 108.25, 107.54, 84.16, 18.01; HRMS (ESI) calculated for $C_{24}H_{18}ON_6I$ $[M + H]^+$ 533.0586; found: 533.0575.

(Z)-5-Methyl-3-((4-methyl-3-((4-pyrdin-3-yl) pyrimidin-2-yl) amino) phenyl) imino) indolin-2-one (7f) White solid (80%); R_f: 0.20 (5% MeOH/$CHCl_3$); M.P.: 134-136 °C; ^{1}H NMR (300 MHz, $CDCl_3$ + DMSO-d_6) δ 10.35 (s, 1H), 9.05 (s, 1H), 8.54 (d, $J = 3.7$ Hz, 1H), 8.36 (d, $J = 5.1$ Hz, 1H), 8.12 (d, $J = 7.9$ Hz, 1H), 7.71 (s, 1H), 7.53 (s, 1H), 7.44 (s, 2H), 7.09 (d, $J = 5.1$ Hz, 1H), 6.95 (d, $J = 7.9$ Hz, 1H), 6.76–6.56 (m, 3H), 2.34 (s, 3H), 1.87 (s, 3H); ^{13}C NMR (75 MHz, $CDCl_3$ + DMSO-d_6) δ 164.72, 162.15, 160.62, 158.86, 154.97, 151.04, 148.41, 148.04, 144.49, 143.87, 138.11, 134.33, 130.96, 126.78, 125.76, 123.33, 113.38, 111.73, 111.08, 107.99, 20.61, 17.71; HRMS (ESI) calculated for $C_{25}H_{21}ON_6$ $[M + H]^+$ 421.1771; found: 421.1763.

(Z)-5-Methoxy-3-((4-methyl-3-((4-pyrdin-3-yl)pyrimidin-2-yl) amino)phenyl)imino)indolin-2-one (7g) White solid (70%); R_f: 0.22 (5% MeOH/$CHCl_3$); M.P.: 132–134 °C; ^{1}H NMR (300 MHz, DMSO-d_6) δ 10.41 (s, 1H), 9.05 (s, 1H), 8.53 (d, $J = 3.7$ Hz, 1H), 8.36 (d, $J = 5.1$ Hz, 1H), 8.12 (d, $J = 7.9$ Hz, 1 H), 7.81 (s, 1H), 7.61 (d, $J = 1.8$ Hz, 1H), 7.54 (d, $J = 3.5$ Hz, 1H), 7.21 (d, $J = 8.1$ Hz, 1H), 7.10 (d, $J = 5.1$ Hz, 1H), 6.72 (s, 2H), 6.62 (dd, $J = 7.9$, 1.8 Hz, 1H), 6.37 (s, 1H), 3.32 (s, 3H), 2.32 (s, 3H); ^{13}C NMR (75 MHz, $CDCl_3$ + DMSO-d_6): δ 164.0, 161.4, 158.2, 153.7, 150.3, 147.4, 147.3, 144.1, 139.8, 137.6, 133.7, 133.6, 130.4, 130.0, 124.5, 122.8, 118.9, 112.8, 111.3, 110.2, 107.3, 54.5, 17.0; HRMS (ESI) calculated for $C_{25}H_{21}O_2N_6$ $[M + H]^+$ 437.1720; found: 437.1714.

(E)-N^1((1*H*-indol-3-yl) methylene)-4-methyl-N^3-(4-(pyridine-3-yl) pyrimidin-2-yl) benzene-1,3-diamine (7h) White solid (74%); R_f: 0.33 (5% MeOH/$CHCl_3$); M.P.: 126–128 °C; ^{1}H NMR (300 MHz, DMSO-d_6) δ 12.12 (s, 1H), 9.87 (s, 1H), 9.23 (s, 1H), 9.00 (s, 1H), 8.66 (s, 1H), 8.47 (dd, $J = 15.9$, 6.4 Hz, 2H), 8.23 (s, 1H), 8.03 (d, $J = 7.0$ Hz, 1H), 7.65–7.50 (m, 2H), 7.44 (s, 2H), 7.29–7.13 (m, 3H), 6.94 (d, $J = 7.3$ Hz, 1H), 2.21 (s, 3H); ^{13}C NMR (100 MHz, DMSO-d_6) δ 185.51, 162.01, 161.18, 160.03, 151.44, 148.18, 139.20, 138.96, 137.52, 135.58, 131.70, 130.81, 130.66, 124.67, 123.94, 122.61, 121.28, 118.31, 112.92, 108.74, 18.18; HRMS (ESI) calculated for $C_{25}H_{21}N_6$ $[M + H]^+$ 405.1822; found: 405.1822.

(E)-N^1((5-Fluoro-1*H*-indol-3-yl)methylene)-4-methyl-N^3-(4-(pyridine-3-yl) pyrimidin-2-yl) benzene-1,3-diamine (7i) White solid (82%); R_f: 0.24 (5% MeOH/$CHCl_3$); M.P.: 146–148 °C; ^{1}H NMR (500 MHz, DMSO-d_6) δ 12.38 (s, 1H), 9.98 (s, 1H), 9.41 (s, 1H), 9.20 (s, 1H), 8.84 (dd, $J =$ 14.3, 4.1 Hz, 1H), 8.72 (d, $J = 7.9$ Hz, 1H), 8.65 (t, $J = 4.6$ Hz, 1H), 8.41 (d, $J = 3.1$ Hz, 1H), 7.81 (dd, $J = 14.2$, 7.3 Hz, 3H), 7.60 (dd, $J = 9.7$, 4.9 Hz, 2H), 7.41 (d, $J = 8.1$ Hz, 1H), 7.19 (dd, $J = 9.2$, 2.5 Hz, 1H), 7.16–7.12 (m, 1H), 2.35 (s, 3H); ^{13}C NMR (100 MHz, DMSO-d_6) δ 185.54, 161.37, 161.29, 161.10, 160.23, 159.16 (d, $J_1 = 234.9$Hz, 1C), 149.61, 146.55, 140.10, 139.32, 139.16, 137.58, 137.40, 134.07, 133.43, 131.78, 131.68, 130.03, 125.47, 119.04, 114.27 (d, $J_3 = 9.7$ Hz, 1C), 112.07 (d, $J_2 = 25.9$Hz, 1C), 108.94, 106.13 (d, $J_2 = 24.5$ Hz, 1C), 18.21; HRMS (ESI) calculated for $C_{25}H_{21}FN_6$ $[M+H]^+$ 423.1732; found: 423.1728.

(E)-3-(((4-Methyl-3-((4-(pyridin-3-yl)pyrimidin-2-yl)amino) phenyl)imino)methyl)-1H-indole-5-carbonitrile (7k) White solid (70 %); R_f: 0.22 (5% MeOH/$CHCl_3$); M.P.: 231–233 °C; ^{1}H NMR (400 MHz, DMSO-d_6) δ 12.78 (s, 1H), 9.98 (s, 1H), 9.47 (s, 1H), 9.24 (s, 1H), 8.98 (d, $J = 7.9$ Hz, 1H), 8.93 (s, 1H), 8.63 (d, $J = 4.9$ Hz, 1H), 8.50 (d, $J = 2.9$ Hz, 1H), 8.44 (s, 1H), 7.99 (dd, $J = 15.0$, 9.4 Hz, 1H), 7.79 (d, $J = 1.4$ Hz, 1H), 7.71 (d, $J = 8.5$ Hz, 1H), 7.66–7.58 (m, 2H), 7.35 (d, $J = 8.1$ Hz, 1H), 7.11 (dd, $J = 8.0$, 1.7 Hz, 1H), 2.28 (s, 3H); ^{13}C NMR (100 MHz, DMSO-d_6) δ 185.97, 161.01, 160.51, 160.07, 146.61, 143.91, 140.77, 139.33, 138.97, 134.60, 131.80, 129.82, 126.89, 126.77, 126.15, 124.41, 120.42, 119.28, 118.42, 114.50, 109.12, 104.82, 18.20; HRMS (ESI) calculated for $C_{25}H_{21}N_6$ $[M+H]^+$ 430.1782; found: 430.1774.

(E)-4-methyl-N^1-((5-nitro-1*H*-indol-3-yl)methylene)-N^1-(4-(pyridine-3-yl)pyrimidin-2-yl)benzene-1,3-diamine (7l) White solid (74%); R_f: 0.20 (5% MeOH/$CHCl_3$); M.P.: 244–245 °C; ^{1}H NMR (300 MHz, $CDCl_3$ + DMSO-d_6) δ 10.04 (s, 1H), 9.31 (d, $J = 2.0$ Hz, 2H), 9.02 (s, 1H), 8.85 (s, 1H), 8.71 (s, 2H), 8.55 (d, $J = 5.1$ Hz, 1H), 8.45 (dd, $J =$ 17.2, 7.1 Hz, 2H), 8.26 (s, 1H), 8.14 (dd, $J = 8.9$, 2.2 Hz, 1H), 7.69 (d, $J = 9.0$ Hz, 1H), 7.59 (t, $J = 3.1$ Hz, 1H), 7.54 (dd, $J = 7.5$, 4.7 Hz, 1H), 7.46 (d, $J = 5.1$ Hz, 1H), 7.38 (d, $J = 5.1$ Hz, 1H), 7.30 (d, $J = 8.1$ Hz, 1H), 7.06 (dd, $J = 8.0$, 1.8 Hz, 1H), 6.89 (d, $J = 8.1$ Hz, 1H), 6.81 (d, $J = 1.9$ Hz,

1H), 6.36 (dd, $J = 8.0$, 2.1 Hz, 1H), 4.95 (s, 1 H), 2.30 (s, 3H); ^{13}C NMR (75 MHz, $CDCl_3 + DMSO\text{-}d_6$) δ 164.0, 161.7, 160.4, 158.5, 153.9, 150.6, 147.7, 147.3, 142.7, 138.1, 133.8, 132.0, 130.8, 123.0, 120.2, 119.8, 115.8, 113.3, 113.0, 112.7, 111.9, 107.6, 17.4; HRMS (ESI) calculated for $C_{25}H_{21}N_6$ $[M + H]^+$ 450.1682; found: 450.1673.

(*E*)-4-methyl-N^3-(4-pyrdin-3-yl)pyrimidin-2-yl)-N^1-((4-trifluoromethylbenzylidene) benzene-1,3-diamine (7n) White solid (85%); $\mathbf{R_f}$: 0.27 (5% MeOH/$CHCl_3$); M.P.: 122–124 °C; ^{1}H NMR (300 MHz, $CDCl_3 + DMSO\text{-}d_6$): δ 9.22 (d, $J = 1.5$ Hz, 1H), 8.63 (dd, $J = 4.8$, 1.4 Hz, 1H), 8.55 (s, 1H), 8.44 (d, $J = 5.2$ Hz, 1H), 8.27 (dd, $J = 6.2$, 1.9 Hz, 1H), 7.98 (d, $J = 8.5$ Hz, 3H), 7.65 (d, $J = 8.1$ Hz, 2H), 7.50 (s, 1H), 7.34 (dd, $J = 7.7$, 4.9 Hz, 1H), 7.19 (d, $J = 8.1$ Hz, 1H), 7.13 (d, $J = 5.2$ Hz, 1H), 6.91 (dd, $J = 8.0$, 2.0 Hz, 1H), 2.31 (s, 3H). ^{13}C NMR (75 MHz, $CDCl_3 + DMSO\text{-}d_6$): δ 162.10, 160.83, 159.12, 158.99, 157.57, 151.24, 149.19, 148.31, 139.46, 138.31, 137.87, 134.31, 132.54, δ 131.88 (q, $J = 32.1$ Hz, 1C), 131.24, 130.93, 130.72, 129.90, 128.92, 128.45, 125.95 (q, $J = 3.6$ Hz, 1C), 125.50, 125.46, 123.88 (q, $J = 272.2$ Hz, 1C), 123.55, 116.84, 115.07, 110.88, 109.61, 107.97, 107.50, 17.88; HRMS (ESI) calculated for $C_{24}H_{19}N_5F_3$ $[M + H]^+$ 434.1582; found: 434.1587.

(*E*)-N^1-(4-fluorobenzylidene)-4-methyl-N^3-(4-pyrdin-3-yl)pyrimidin-2-yl)benzene-1,3-diamine (7o) White solid (75%); R_f: 0.32 (5% MeOH/$CHCl_3$); M.P.: 138–140 °C; ^{1}H NMR (300 MHz, $CDCl_3 + DMSO\text{-}d_6$): δ 9.20 (s, 1H), 8.62 (s, 1H), 8.45 (s, 1H), 8.28 (d, $J = 5.5$ Hz, 1H), 7.97 (s, 2H), 7.85 (s, 1H), 7.50 (m, 2H), 7.20–6.97 (m, 5H), 6.88 (s, 1H), 2.30 (s, 3H); ^{13}C NMR (75 MHz,$CDCl_3 + DMSO\text{-}d_6$): δ 167.48, δ 164.44 (d, $J_1 = 252.2$ Hz), 162.35, 160.73, 159.06, 158.12, 151.24, 149.99, 148.31, 138.04, 134.52, 132.65, 132.26, 130.94, 130.68, 127.26, 127.02, 123.64, 116.73, 116.29 (d, $J_2 = 22.6$ Hz), 115.93, 115.64, 115.37, 115.08, 114.27, 110.92, 109.12, 17.79; MS–ESI-MS: *m/z* 384 HRMS (ESI) calculated for $C_{25}H_{21}N_6O$ $[M + H]^+$ 384.1626; found: 384.1619.

Biology

Cell cultures, maintenance, and evaluation of anti-proliferative activity

Cell line utilized during the experiments was procured from American Type Culture Collection (ATCC, USA), K562 cells were grown in RPMI1640 medium at 37 °C containing 10% Fetal Bovine Serum (FBS). The cells were collected after 24 h post treatment. To estimate the cell growth in the presence of the compounds, SRB cell proliferation assay was performed. In a 96 well plate, cell line was seeded in media containing 10% FBS and based on the cells replicative capacity, plating was performed. Prior to treatment with experimental drugs, plates were maintained at 100% relative humidity, 5% CO_2, 95% air and temperature of 37 °C. To each well, 198 µL of medium containing cells and 2 µL of test compounds were added. The assay was performed in triplicates for each sample and five different concentrations (0.01, 0.1, 1, 10, and 100 µM) were taken into consideration. After incubation for 24 h, 100 µL of ice-cold 10% TCA was added and incubated at 40 °C for 60 min. Post-incubation plates were washed thrice with water and dried at room temperature.

To each well, 100 µL of SRB (sulforhodamine B) solution was added and incubated at room temperature for 30 min. Plates were washed with 1% acetic acid thrice to remove unbound dye and left for drying overnight. A volume of 200 µl of 10 mM Tris base solution was added to each well to solubilize the protein bound dye and measurements were taken at 510 nm with aid of Varioscan Flash multimode plate reader. Based on the percentage growth in controls, the inhibitory concentrations were determined and graphs were plotted between percentage of viable cells and concentration of compounds. IC_{50} values were calculated and reported as result of mean ± SD for all triplicate independent experiments.

BCR-ABL kinase inhibitory assay

The kinase inhibitory effect of the test compounds was assessed by Z-lyte kinase assay kit (details) according to manufacturer's instructions which is based on the differential sensitivity of phosphorylated and non-phosphorylated peptides to proteolytic cleavage. Test compounds with 5 mM concentrations was diluted to 1000 µM with DMSO and transferred to the dose plate. Further, each compound was diluted to 10-fold concentration with reaction buffer to obtain a 10X final concentration. Later, the compounds (1 µL/well) were transferred to assay plate with a concentration ranging from 100 to 0.006 µM for the BCR-ABL activity. Imatinib was run in parallel as a positive control. Reaction mixture with ATP (0% inhibition), without ATP (100% inhibition) and without ATP and kinase peptide mixture (100% phosphorylation) are used as controls in the experiments. The reaction mixtures were mixed and incubated 1 h at room temperature followed by development reaction. All the plates were incubated at room temperature for 1 h and the fluorescence signal was measured at an excitation and emission wavelengths of 400 and 445 nm, respectively. Each experiment was performed in triplicates and the results are expressed as mean ± S.D.

Molecular docking studies

All computational calculations were carried out on an Intel (R) Xenon(R) 2 Duo CPU E7600 @ 3.06 GHz processor with memory of 2 GB RAM running with the LINUX operating system. Software package used was Schrodinger suite 2017 drug discovery suite. Docking (Friesner et al. 2006) studies were perfomed for dataset compounds on to the active site of Bcr-Abl crystal structure (PDB ID: 3CS9) using Schrodinger Suite 2017. Structures were sketched and converted to 3D using Ligprep (Schrödinger 2014). Bcr-Abl crystal structure was prepared using Protein Prep wizard, Schrodinger Suite. Further grid was defined using center of nilotinib co-crystal as reference. Top 10 docking poses for each compound was generated and analyzed. Manual inspection of hits was performed to understand the binding pattern and docking scores were considered.

X-ray crystallography 7l

X-ray data for the compound **7l** was collected at room temperature on a Bruker D8 QUEST instrument with an IμS Mo microsource ($\lambda = 0.7107$ A) and a PHOTON-100 detector. The raw data frames were reduced and corrected for absorption effects using the Bruker Apex 3 software suite programs (Bruker 2016). The structure was solved using intrinsic phasing method and further refined with the SHELXL program and expanded using Fourier techniques (Sheldrick 2015). Anisotropic displacement parameters were included for all non-hydrogen atoms. N bound H atom was located in difference Fourier maps and their positions and isotropic displacement parameters were refined. All other C bound H atoms were positioned geometrically and treated as riding on their parent C atoms [C–H = 0.93–0.97 Å, and $U_{iso}(H) = 1.5U_{eq}(C)$ for methyl H or $1.2U_{eq}(C)$ for other H atoms]. The crystal was found to be twinned and the exact twin matrix was identified by the integration program as 0.989 0.011 −0.021, 0 −1 0, −0.995 −0.006 −0.989. The structure was refined using the hklf 5 routine with all reflections.

Crystal data for 7a $C_{24}H_{18}N_6O$ (M = 406.44 g/mol): triclinic, space group P-1 (no. 2), $a = 8.46500(10)$ Å, $b = 11.00000(10)$ Å, $c = 11.4730(3)$ Å, $\alpha = 70.5200(6)°$, $\beta = 80.6100(6)°$, $\gamma = 89.3400(7)°$, $V = 992.60(3)$ Å^3, $Z = 2$, $T = 294.15$ K, μ(MoKα) = 0.088 mm-1, $D_{calc} = 1.360$ g/cm^3, 11,518 reflections measured ($4.468° \le 2\Theta \le 50°$), 11518 unique ($R_{int} = ?$, $R_{sigma} = 0.0976$) which were used in all calculations. The final R_1 was 0.0813 ($I > 2\sigma(I)$) and wR_2 was 0.2450 (all data). CCDC 1841348 contains supplementary Crystallographic data for the structure. These data can be obtained free of charge at www.ccdc.cam.ac.uk/conts/retrieving.html [or from the Cambridge Crystallographic Data Centre (CCDC), 12 Union Road, Cambridge CB2 1EZ, UK; fax: +44(0) 1223 336 033; email: deposit@ccdc.cam.ac.uk].

Acknowledgements The author AR thanks CSIR and UGC, New Delhi for the award of fellowships. The author RS thanks CSIR-HRDG for the award of CSIR-SRAship (13(8906-A)/2017-pool).

Compliance with ethical standards

Conflict of interest The authors declare that they have no conflict of interest.

References

Amala K, Bhujanga Rao AK, Gorantla B, Gondi CS, Rao JS (2013) Design, synthesis and preclinical evaluation of NRC-AN-019. Int J Oncol 42:168–178

An X, Tiwari AK, Sun Y, Ding PR, Ashby Jr. CR, Chen ZH (2010) BCR-ABL tyrosine kinase inhibitors in the treatment of Philadelphia chromosome positive chronic myeloid leukemia: a review. Leuk Res 34:1255–1268

Ateyya H, Hassan ZA, El-Sherbeeny NA (2017) The selective tyrosine kinase-inhibitor nilotinib alleviates experimentally induced cisplatin nephrotoxicity and hepatotoxicity. Environ Toxicol Pharmacol 55:60–67

Azevedo AP, Reichert A, Afonso C, Alberca MD, Tavares P, Lima F (2017) BCR-ABL V280G mutation, potential role in Imatinib resistance: first case report. Clin Med Insights Oncol 11:1–5

Banavath HM, Sharma OP, Kumar MS, Baskaran R (2014) Identification of novel tyrosine kinase inhibitors for drug resistant T315I mutant BCR-ABL: a virtual screening and molecular dynamics simulations study. Sci Rep 4:6948

Bruker (2016) APEX SAINT and SADABS. Bruker AXS, Inc, Madison, Wisconsin, USA

Carter BZ, Mak PY, Mu H, Zhou H, Mak DH, Schober W, Leverson JD, Zhang B, Ravi B, Xuelin H, Cortes J, Hagop K, Marina K, Andreeff M (2016) Combined targeting of BCL-2 and BCR-ABL tyrosine kinase eradicates chronic myeloid leukemia stem cells. Sci Transl Med 8:1–24

Chatree C-A, Wilson L, Christopher H (2016) Major arterial events in patients with chronic myeloid leukemia treated with tyrosine kinase inhibitors: a meta-analysis. Leuk Lymphoma 57:1300–1310

Cortes JE, Hochhaus A, le Coutre PD, Rosti G, Pinilla-Ibarz J, Jabbour E, Gillis K, Woodman RC, Blakesley RE, Giles FJ, Kantarjian HM, Baccarani M (2011) Minimal cross-intolerance with nilotinib in patients with chronic myeloid leukemia in chronic or accelerated phase who are intolerant to imatinib. Blood 117:5600–5606

Cortes JE, Saglio G, Kantarjian HM, Baccarani M, Mayer J, Boqué C, Shah NP, Chuah C, Casanova L, Bradley-Garelik B, Manos G, Hochhaus A (2016) Final 5-year study results of DASISION: the Dasatinib versus Imatinib study in treatment-naïve chronic myeloid leukemia patients trial. J Clin Oncol 34:2333–2340

Dahlen T, Edgen G, Lambe M, Hoglund M, Bjorkholm M, Sandin F, Sjalander A, Richter J, Olsson-Stromberg U, Ohm L, Back M, Stenke L, Swedish CML, Group and the Swedish CML Register Group (2016) Cardiovascular events associated with use of tyrosine kinase inhibitors in chronic myeloid leukemia: a population-based cohort study. Ann Intern Med 165:161–166

Daina A, Michielin O, Zoete V (2017a) SwissADME: a free web tool to evaluate pharmacokinetics, drug-likeness and medicinal chemistry friendliness of small molecules. Sci Rep 7:42717

Daina A, Michielin O, Zoete V (2017b) SwissADME: a free web tool to evaluate pharmacokinetics, drug-likeness and medicinal chemistry friendliness of small molecules. Sci Rep 7:1–13

Ding Wu, Mand MR, Veach DR, Parker LL, Clarkson B, Kron SJ (2008) A solid-phase Bcr-Abl kinase assay in 96-well hydrogel plates. Anal Biochem 375:18–26

Druker BJ (2003) Imatinib alone and in combination for chronic myeloid leukemia. Semin Hematol 40:50–58

El Sayed MT, Hamdy NA, Osman DA et al. (2015) Indoles as anticancer agents. Adv ModOncol Res 1:20–35

Friesner RA, Murphy RB, Repasky MP, Frye LL, Greenwood JR, Halgren TA, Sanschagrin PC, Mainz DT (2006) Extra precision glide: docking and scoring incorporating a model of hydrophobic enclosure for protein-ligand complexes. J Med Chem 49:6177–6196

Gambacorti-Passerini C, Brümmendorf TH, Kim DW, Turkina AG, Masszi T, Assouline S, Durrant S, Kantarjian HM, Khoury HJ, Zaritskey A, Shen ZX, Jin J, Vellenga E, Pasquini R, Mathews V, Cervantes F, Besson N, Turnbull K, Leip E, Kelly V, Cortes JE (2014) Bosutinib efficacy and safety in chronic phase chronic myeloid leukemia after imatinib resistance or intolerance: minimum 24-month follow-up. Am J Hematol 89:732–742

Giles FJ, le Coutre PD, Pinilla-Ibarz J, Larson RA, Gattermann N, Ottmann OG, Hochhaus A, Radich JP, Saglio G, Hughes TP, Martinelli G, Kim DW, Novick S, Gillis K, Fan X, Cortes J, Baccarani M, Kantarjian HM (2013) Nilotinib in imatinib-resistant or imatinib-intolerant patients with chronic myeloid leukemia in chronic phase: 48-month follow-up results of a phase II study. Leukemia 27:107–112

Goldman JM, Melo JV (2008) BCR-ABL in chronic myelogenous leukemia--how does it work? Acta Haematol 119:212–217

Gusarova GA, Turkina AG (2016) Arterial events in patients with chronic myeloid leukemia receiving treatment with second generation tyrosine kinase inhibitors. Clin Oncohematology 9:474–484

Haguet H, Douxfils J, Mullier F, Chatelain C, Graux C, Dogné J-M (2017) Belg J Hematol 8:45

Hamaï A, Richon C, Meslin F, Faure F, Kauffmann A, Lecluse Y, Jalil A, Larue L, Avril MF, Chouaib S, Mehrpour M (2006) Imatinib enhances human melanoma cell susceptibility to TRAIL-induced cell death: relationship to Bcl-2 family and caspase activation. Oncogene 25:7618–1734

Havrylyuk D, Kovach N, Zimenkovsky B, Vasylenko O, Lesyk R (2011) Synthesis and anticancer activity of isatin-based pyrazolines and thiazolidines conjugates. Arch Pharm 344:514–522

Herrmann J (2016) Tyrosine kinase inhibitors and vascular toxicity: impetus for a classification system? Curr Oncol Rep 18:33

Hochhaus A, Baccarani M, Deininger M, Apperley JF, Lipton JH, Goldberg SL, Corm S, Shah NP, Cervantes F, Silver RT, Niederwieser D, Stone RM, Dombret H, Larson RA, Roy L, Hughes T, Müller MC, Ezzeddine R, Countouriotis AM, Kantarjian HM (2008) Dasatinib induces durable cytogenetic responses in patients with chronic myelogenous leukemia in chronic phase with resistance or intolerance to imatinib. Leukemia 22:1200–1206

Hochhaus A, Saglio G, Hughes TP, Larson RA, Kim DW, Issaragrisil S, le Coutre PD, Etienne G, Dorlhiac-Llacer PE, Clark RE, Flinn IW, Nakamae H, Donohue B, Deng W, Dalal D, Menssen HD, Kantarjian HM (2016) Long-term benefits and risks of frontline nilotinib vs imatinib for chronic myeloid leukemia in chronic phase: 5-year update of the randomized ENESTnd trial. Leukemia 30:1044–1054

Hu Y, Kunimoto R, Bajorath J (2017) Mapping of inhibitors and activity data to the human kinome and exploring promiscuity from a ligand and target perspective. Chem Biol Drug Des 89:834–845

Hughes T, Saglio G, Branford S, Soverini S, Kim DW, Müller MC, Martinelli G, Cortes J, Beppu L, Gottardi E, Kim D, Erben P, Shou Y, Haque A, Gallagher N, Radich J, Hochhaus A (2009) Impact of baseline BCR-ABL mutations on response to nilotinib in patients with chronic myeloid leukemia in chronic phase. J Clin Oncol 27:4204–4210

Jabbour E, Jones D, Kantarjian HM, O'Brien SG, Tam C, Koller C, Burger JA, Borthakur G, Wierda WG, Cortes J (2009) Long-term outcome of patients with chronic myeloid leukemia treated with second-generation tyrosine kinase inhibitors after imatinib failure is predicted by the in vitro sensitivity of BCR-ABL kinase domain mutations. Blood 114:2037–2043

Jason G (2017) Tyrosine kinase inhibitors in the treatment of eosinophilic neoplasms and systemic mastocytosis. Hemato Oncol Clin N Am 31:643–661

Jonathan D, Helene H, Francois M et al. (2016) Association between BCR-ABL tyrosine kinase inhibitors for chronic myeloid leukemia and cardiovascular events, major molecular response, and overall survival a systematic review and meta-analysis. JAMA Oncol 2:625–632

Kang CM, Liu DQ, Zhao XH, Dai YJ, Cheng JG, Lv YT (2016) QSAR and molecular docking studies on oxindole derivatives as VEGFR-2 tyrosine kinase inhibitors. J Recept Signal Transduct Res 36:103–109

Kantarjian H, Pasquini R, Hamerschlak N, Rousselot P, Holowiecki J, Jootar S, Robak T, Khoroshko N, Masszi T, Skotnicki A, Hellmann A, Zaritsky A, Golenkov A, Radich J, Hughes T, Countouriotis A, Shah N (2007) Dasatinib or high-dose imatinib for chronic-phase chronic myeloid leukemia after failure of first-line imatinib: a randomized phase 2 trial. Blood 109:5143–5150

Kantarjian HM, Cortes JE, Kim DW, Khoury HJ, Brümmendorf TH, Porkka K, Martinelli G, Durrant S, Leip E, Kelly V, Turnbull K, Besson N, Gambacorti-Passerini C (2014) Bosutinib safety and management of toxicity in leukemia patients with resistance or intolerance to imatinib and other tyrosine kinase inhibitors. Blood 123:1309–1318

Karl Peggs MA, Stephen Mackinnon MD (2003) Imatinib Mesylate—The new gold standard for treatment of chronic myeloid leukemia. N Engl J Med 348:1048–1050

Kasinski AL, Kelnar K, Stahlhut C, Orellana E, Zhao J, Shimer E, Dysart S, Chen X, Bader AG, Slack FJ (2015) A combinatorial microRNA therapeutics approach to suppressing non-small cell lung cancer. Oncogene 34:3547–3555

Kaur M, Singh M, Chadha N, Silakari O (2016) Oxindole: a chemical prism carrying plethora of therapeutic benefits. Eur J Med Chem 123:858–894

Lipton JH, Chuah A, Guerci-Bresler A, Rosti G, Simpson D, Assouline S, Etienne G, Nicolini FE, le Coutre PD, Clark RE, Stenke L, Andorsky D, Oehler V, Lustgarten S, Rivera VM, Clackson T, Haluska FG, Baccarani M, Cortes JE, Guilhot F, Hochhaus A, Hughes T, Kantarjian HM, Shah NP, Talpaz M, Deininger MW (2016) Ponatinib versus imatinib for newly diagnosed chronic myeloid leukaemia: an international, randomised, open-label, phase 3 trial. Lancet Oncol 17:612–621

Manning G, Whyte DB, Martinez R, Hunter T, Sudarsanam S (2002) The protein kinase complement of the human genome. Science 298:1912–1934

Milojkovic D, Apperley JF, Gerrard G, Ibrahim AR, R. Szydlo R, Bua M, Reid A, Rezvani K, Foroni L, Goldman J, Marin D (2012) Responses to second-line tyrosine kinase inhibitors are durable: an intention-to-treat analysis in chronic myeloid leukemia patients. Blood 119:1838–1843

Mow BM, Chandra J, Svingen PA, Hallgren CG, Weisberg E, Kottke TJ, Narayanan VL, Litzow MR, Griffin JD, Sausville EA, Tefferi A, Kaufmann SH (2002) Effects of the Bcr/abl kinase inhibitors STI571 and adaphostin (NSC 680410) on chronic myelogenous leukemia cells in vitro. Blood 99:664–671

Nicolini FE, Basak GW, Kim DW, Olavarria E, Pinilla-Ibarz J, Apperley JF, Hughes T, Niederwieser D, Mauro MJ, Chuah C, Hochhaus A,

Martinelli G, DerSarkissian M, Duh MS, McGarry LJ, Kantarjian HM, Cortes JE (2017) Overall survival with ponatinib versus allogeneic stem cell transplantation in Philadelphia chromosome-positive leukemias with the T315I mutation. Cancer 123:2875–2880

Nida I, Naveed I (2014) Imatinib: a breakthrough of targeted therapy in cancer. Chemother Res Pract 2014:1–9

O'Hare T, Eide CA, Deininger MW (2007) Bcr-Abl kinase domain mutations, drug resistance and the road to a cure for chronic myeloid leukemia. Blood 110:2242–2249

Oren P, Avi L, Zaza I, Yishay W, Ran K, Pia R (2015) Tyrosine kinase inhibitor associated vascular toxicity in chronic myeloid leukemia. Cardio-Oncol 1:1–10

Ouellette SB, Noel BM, Parker LL (2016) A cell-based assay for measuring endogenous BcrAbl kinase activity and inhibitor resistance PLoS ONE 11:e0161748

Parcha P, Sarvagalla S, Madhuri B, Pajaniradje S, Baskaran V, Coumar MS, Rajasekaran B (2017) Identification of natural inhibitors of Bcr-Abl for the treatment of chronic myeloid leukemia. Chem Biol Drug Des 90:596–608

Porkka K, Koskenvesa P, Lundán T, Rimpiläinen J, Mustjoki S, Smykla R, Wild R, Luo Arnan M, Brethon B, Eccersley L, Hjorth-Hansen H, Höglund M, Klamova H, Knutsen H, Parikh S, Raffoux E, Gruber F, Brito-Babapulle F, Dombret H, Duarte RF, Elonen E, Paquette R, Zwaan CM, Lee FY (2008) Dasatinib crosses the blood-brain barrier and is an efficient therapy for central nervous system Philadelphia chromosome-positive leukemia. Blood 112:1005–1012

Prakash B, Amuthavalli A, Edison D, Sivaramkumar MS, Velmurugan R (2018) Synthesis of novel 3,5-disubstituted-2-oxindole derivatives as antitumor agents against human non-small cell lung cancer. Med ChemResearch 27:321–331

Płużański A, Piórek A (2016) Side effects of tyrosine kinase inhibitors-management guidelines. Oncol Clin Pract 12:113–118

Rebecca M, Lisa EMH, Pablo B, Elaine KA, Kay H, Daniel J, Graham H, Arunima M, Jim O, Alan H, Melo JV, Edmond C, Kevin MR, Véronique M-S, Brian JD, Richard EC, Subir M, Pawel H, Franck EN, Paolo S, Emma S, Bruno C, Tessa LH, Helgason GV (2018) Targeting BCR-ABL-independent TKI resistance in chronic myeloid leukemia by mTOR and autophagy inhibition. J Natl Cancer Inst 110:467–478

Sabitha K (2012) Nilotinib based pharmacophore models for BCRABL. Bioinformation 8:658–663

Salesse S, Verfaillie CM (2002) BCR/ABL: from molecular mechanisms of leukemia induction to treatment of chronic myelogenous leukemia. Oncogene 21:8547–8559

Sawyers CL, Hochhaus A, Feldman E, Goldman JM, Miller CB, Ottmann OG, Schiffer CA, Talpaz M, Guilhot F, Deininger MW, Fischer T, O'Brien SG, Stone R, Gambacoti-Passerini CB, Russel NH, Reiffers JJ, Shea TC, Chapuis B, Coutre S, Tura S, Morra E, Larson RA, Saven A, Peschel C, Gratwohl A, Mandelli F, Ben-Am M, Gathmann I, Capdeville R, Paquette RL, Druker BJ (2002) Imatinib induces hematologic and cytogenetic responses in patients with chronic myelogenous leukemia in myeloid blast crisis: results of a phase II study. Blood 99:3530–3539

Schrödinger (2014) LigPrep version 3.2 LLC, New York, NY

Shah NP, Guilhot F, Cortes JE, Schiffer CA, le Coutre P, Brümmendorf TH, Kantarjian HM, Hochhaus A, Rousselot P, Mohamed H, Healey D, Cunningham M, Saglio G (2014) Long-term outcome with dasatinib after imatinib failure in chronic-phase chronic myeloid leukemia: follow-up of a phase 3 study. Blood 123:2317–2324

Sheldrick GM (2015) Crystal structure refinement with SHELXL. Acta Crystallogr Sect CStructural Chem 71:3–8

Sidhu JS, Singla R, Mayank, Jaitak V (2015) Indole derivatives as anticancer agents for breast cancer therapy: a review. Anticancer Agents Med Chem 16:160–173

da Silva MM, Comin M, Duarte TS, Foglio MA, de Carvalho JE, do Vieira MC, Formagio AS (2015) Synthesis, antiproliferative activity and molecular properties predictions of galloyl derivatives. Molecules 20:5360–5373

Skehan P, Storeng R, Scudiero D, Monks A, McMahon J, Vistica D, Warren JT, Bokesch H, Kenney S, Boyd MR (1990) New colorimetric cytotoxicity assay for anticancer-drug screening. J Natl Cancer Inst 82:1107–1112

Sodergren SC, White A, Efficace F, Sprangers M, Fitzsimmons D, Bottomley A, Johnson CD (2014) Systematic review of the side effects associated with tyrosine kinase inhibitors used in the treatment of gastrointestinal stromal tumours on behalf of the EORTC Quality of Life Group. Crit Rev Oncol Hematol 91:35–46

Staquinini FI, Qian MD, Salameh A, Dobroff AS, Edwards JK, Cimino DF, Moeller BJ, Kelly P, Nunez MI, Tang X, Liu DD, Lee JJ, Hong WK, Ferrara F, Bradbury ARM, Lobb RR, Edelman MJ, Sidman RL, Wistuba II, Arap W, Pasqualini R (2015) Receptor tyrosine kinase EphA5 is a functional molecular target in human lung cancer. J Biol Chem 290:7345–7359

Talpaz M, Silver RT, Druker BJ, Goldman JM, Gambacoti-Passerini CB, Guilhot F, Schiffer CA, Fischer T, Deininger MW, Lennard AL, Hochhaus A, Ottmann OG, Gratwohl A, Baccarani M, Stone R, Tura S, Mahon FX, Fernandes-Reese S, Gathmann I, Capdeville R, Kantarjian HM, Sawyers CL (2002) Imatinib induces durable hematologic and cytogenetic responses in patients with accelerated phase chronic myeloid leukemia: results of a phase 2 study. Blood 99:1928–1937

Teng Y-O, Zhao H-Y, Wang J, Liu H, Gao M-L, Zhou Y, Han K-L, Fan Z-C, Zhang Y-M, Sun H, Yu P (2016) Synthesis and anticancer activity evaluation of 5-(2-carboxyethenyl)-isatin derivatives. Eur J Med Chem 112:145–156

Valent P (2007) Imatinib-resistant chronic myeloid leukemia (CML): current concepts on pathogenesis and new emerging pharmacologic approaches. Biologics 1:433–448

Valent P (2011) Severe adverse events associated with the use of second-line BCR/ABL tyrosine kinase inhibitors: preferential occurrence in patients with comorbidities. Haematol 96:1395–1397

Vichai V, Kirtikara K (2006) Sulforhodamine B colorimetric assay for cytotoxicity screening. Nat Protoc 1:1112–1116

Vine KL, Matesic L, Locke JM, Ranson M, Skropeta D (2009) Cytotoxic and anticancer activities of isatin and its derivatives: a comprehensive review from 2000–2008. Anticancer Agents Med Chem 9:397–414

Vine KL, Matesic L, Locke JM, Skropeta D (2013) Recent highlights in the development of isatin-based anticancer agents. Adv Anticancer Agents Med Chem 59:254–312

Wilhelm SM, Carter C, Tang L, Wilkie D, McNabola A, Rong H, Chen C, Zhang X, Vincent P, McHugh M, Cao Y, Shujath J, Gawlak S, Eveleigh D, Rowley B, Liu L, Adnane L, Lynch M, Auclair D, Taylor I, Gedrich R, Voznesensky A, Riedl B, Post LE, Bollag G, Trail PA (2004) BAY 43-9006 exhibits broad spectrum oral antitumor activity and targets the RAF/MEK/ERK pathway and receptor tyrosine kinases involved in tumor progression and angiogenesis. Cancer Res 64:7099–8109

Zimmermann J EP Patent (1993) Pyrimidin derivatives and process for their preparation. PT564409

Zimmermann J (1996) US Patent Pyrimidine derivatives and processes for the preparation thereof. 5521184

Zimmermann J, Buchdunger E, Mett H, Meyer T, Lydon NB, Traxler P (1996) Phenylamino-pyrimidine (PAP)-derivatives: a new class of potent and highly selective PDGF-receptor autophosphorylation inhibitors. Bioorg Med Chem Lett 11:1221–1226

Zámečníkova A (2010) Targeting the BCR-ABL tyrosine kinase in chronic myeloid leukemia as a model of rational drug design in cancer. Expert Rev Hematol 3:45–56